

Dispersion and Subsidence of the Exhaust of a Supersonic Transport in the Stratosphere

Thomas J. Overcamp* and James A. Fay†
MIT, Cambridge, Mass.

A theoretical model is presented that describes the early time history of the wake of an aircraft. This theory shows that far downstream of the aircraft, buoyancy dominates the growth of the wake. For a supersonic transport flying in the stratosphere, the stable stratification will limit the growth of the wake. Data of the visible width of the wake from laboratory experiments in a towing tank and from studies on the growth of contrails from subsonic aircraft verify the model for a neutral atmosphere. A model is developed to show that the exhaust gases of a supersonic transport can sink due to differential radiative cooling caused by the high concentration of water vapor and the lower concentration of ozone in the wake. Estimates of the rate of subsidence are given for aircraft flying between 16 and 27 km.

I. Introduction

IN recent years there has been considerable concern that the engine emissions of a projected fleet of supersonic transports (SST) will destroy a significant fraction of the ozone in the stratosphere. Since this ozone absorbs most of the solar ultraviolet radiation, which may cause skin cancer, any change in the total amount of ozone in the stratosphere could have serious consequences for man.

Johnston^{1,2} developed a photochemical model for ozone that showed that the oxides of nitrogen (NO_x) emitted by the SST's may reduce the total amount of ozone. His model assumed that the NO_x emitted by a proposed fleet would be distributed throughout various arbitrary layers in the stratosphere with an average residence time ranging from six months at 15 km to two years above 20 km. His calculations showed that the total ozone would diminish by as much as a factor of two.

Johnston's report has met with criticism which falls in two basic areas: the uncertainty of his photochemical model and his neglect of the details of the atmospheric transport processes. The chemical model contains many reactions with unknown rate constants, in particular the reactions that convert the NO_x into less harmful molecules. The transport processes, on the other hand, are felt to be important because the time constants for the reactions are very long for altitudes of 20 km or less. Since this is the region in which the first generation SST's, the Anglo-French Concorde and the Soviet Tupolev 144, now fly, transport processes could dominate the proposed NO_x photochemistry and prevent the destruction of ozone. For a brief summary of the arguments pertaining to these questions, see *Inadvertent Climate Modification*.³

This paper examines the initial dispersion of the exhaust products caused by the turbulence and buoyant forces in the aircraft's wake. It shows that the stable stratification of the stratosphere limits the growth of the wake. Since the atmospheric turbulence in the stratosphere is relatively weak, further dispersion should be slow. Therefore each exhaust trail may remain a distinct entity for periods of hours to days or longer.

This conclusion leads to speculation on the fate of such an exhaust trail. Since it would have a high NO_x concentration, photochemical reactions may locally deplete the ozone resulting in a lower level of solar heating due to absorption of ultraviolet radiation. Also excess water vapor in the trail would cause increased radiational cooling in the far infrared bands. These combined effects would cause the trail to cool relative to the surrounding air and sink. If this subsidence could dramatically shorten the residence time of the NO_x in the stratosphere, it would decrease the average reduction of ozone and, thereby, reduce the environmental impact of a fleet of supersonic transports.

The calculations in this paper show that at the cruise altitudes of the first generation SST's, there will be little, if any, subsidence. For aircraft flying at higher altitudes, 27 km for example, the exhaust gases could sink several kilometers in the course of a week if the dispersion of the exhaust products by atmospheric turbulence is small.

Section II presents the theoretical models and their appropriate scaling lengths used to describe the growth of the wake. Data from model experiments of an aircraft wake in a towing tank and data from observations of contrails of subsonic aircraft are compared to the theoretical models in Sec. III. In Sec. IV a model to calculate wake subsidence is developed for aircraft flying in the stratosphere. Our conclusions are in Sec. V.

II. Theoretical Analysis of Wake Growth

The mechanisms that promote the dispersion of the exhaust of a jet aircraft are; 1) the mechanical turbulence in the aircraft's wake, 2) the buoyancy induced turbulence due to the excess temperature of the exhaust gases, and 3) atmospheric turbulence. The stability of the atmosphere gradually inhibits the dispersion by damping turbulent fluctuations and limiting the rise and growth of the exhaust due to its own buoyancy.

Several recent papers have treated the region of the wake dominated by the trailing vortex pair. Crow⁴ showed that this trailing vortex pair was unstable because of mutual and self-induction of the vortices. This theory appears to explain the sinusoidal instability of the vortices that can frequently be observed for high-flying aircraft when their contrails mark their vortex cores.

Scorer and Davenport,⁵ Tombach,⁶ and Saffman⁷ have presented theories on the motion of vortex pairs in a stratified atmosphere. At the present, there is no quantitative evidence to verify any of these theories.

Heywood, Fay, and Linden⁸ proposed an entrainment theory modeling the growth of the aircraft exhaust. This theory, which neglects the vortex pair and atmospheric

Presented as Paper 72-650 at the AIAA 5th Fluid and Plasma Dynamics Conference, Boston, Mass., June 26-28, 1973; submitted December 5, 1972; revision received August 23, 1973. This research was partially sponsored under NASA Grant NGL 22-009-378. We acknowledge discussions with S. E. Widnall and R. Prinn, and the use of the towing tank of the Department of Ocean Engineering of the Massachusetts Institute of Technology.

Index categories: Jets, Wakes, and Viscid-Inviscid Flow Interactions; Atmospheric, Space, and Oceanographic Sciences.

*NSF Fellow. Presently at the Meteorology Program, University of Maryland.

†Professor of Mechanical Engineering. Fellow AIAA.

stratification, showed that close to the aircraft the buoyant wake's growth resembles the growth of an axisymmetric wake, i.e., its width increases with $x^{1/3}$ where x is the downstream distance from the aircraft. Far from the aircraft, buoyancy dominates the flow causing the wake to resemble a line thermal whose width and rise grow proportionately to $x^{2/3}$.

This research shows the relative contributions of the vortex pair and the buoyancy of the exhaust gases on the growth of the wake of the aircraft. The following analysis presents theoretical models with appropriate scaling lengths that are used to describe the wake in both stratified and unstratified atmospheres.

Analysis of the Wake in an Unstratified Atmosphere

For this analysis, it is convenient to divide the wake into three characteristic regimes. The *near wake* is the region close to the aircraft where the separate exhaust streams grow by entraining the surrounding air but are not appreciably influenced by the downwash. Also in the near wake there exist separate regions of axial velocity defect (thrust and drag) that have not counteracted one another. The *intermediate wake* is the region dominated by the trailing vortex pair formed by the circulation, a consequence of lift. The engine exhaust streams are entrained into the vortex system and are wrapped around the vortex cores. The *far wake* begins with the breakup of the vortex system, erasing the memory of the orderly wake upstream. The unbalanced buoyancy forces, resulting from the exhaust heat, dominate the subsequent motion since all other forces decrease in intensity. In an unstratified atmosphere, these buoyancy forces will cause a continual rising and growth of the wake.

The following definitions clarify the terminology used in this analysis. The heat flow H added to the wake is

$$H \equiv m_j \left[c_p (T_j - T) + \frac{1}{2} (v_j^2 - v^2) \right] \quad (1)$$

in which m_j is the total mass flow through the engines, T_j and T are exhaust and freestream temperature, and v_j and v are the exhaust and freestream velocities respectively.

The propulsive thrust, equal to the drag D , is

$$D \equiv m_j (v_j - v) \quad (2)$$

We relate the heat flow H and drag D with the definition of the over-all propulsive efficiency, η

$$\eta \equiv Dv/H \quad (3)$$

Since all reported observations show that the exhaust gases are entrained into the vortex system, we did not feel it necessary to make detailed models for the near wake. The exact flow will depend on the configuration of the aircraft.

In the intermediate region, the flow should closely resemble the classical, infinite vortex pair. This pair propels itself downward with a velocity of $\Gamma/(2\pi s')$ where Γ is the circulation about one of the vortices and s' is the vortex spacing, which is slightly less than the wing span s (being equal to $(\pi s/4)$ for an elliptical wing loading). This pair convects with it an elliptical region of width $2.09s'$ and height $1.73s'$. All the fluid outside of the vortex cores is irrotational.⁹

The exhaust jet will gradually fill this elliptical region due to the turbulence remaining in the wake and the flow swirling about the vortex cores. Except for this decaying turbulence, the flow is essentially irrotational, and the entrainment should be slow and may essentially cease after the exhaust fills this region. Therefore, it is expected that the characteristic radial scaling length is the vortex spacing s' , or as a simplification, the wing span s .

The flow in the intermediate wake is characterized by a time τ_c

$$\tau_c \equiv (2\pi\Gamma/s'^2) \cong (2\pi\rho v s^3/L) \quad (4)$$

in which L is the lift and ρ is the freestream density. This is the time defined by Crow⁴ for the sinusoidal instability. We prefer to use a characteristic distance d_c

$$d_c = (2\pi\rho v^2 s^3/L) \quad (5)$$

Using flight data on several airplanes, Condit and Tracy¹⁰ have shown that the pair breaks up in about $2.2d_c$. Since d_c varies from 3 to 10 km for commercial aircraft, the length of the intermediate region will range up to 20 km.

The breakup of the vortex pair destroys the orderly flow pattern of the intermediate wake. Gradually the buoyant forces in the wake overcome the original downward momentum of the wake and reverse the over-all flow. Buoyancy induced vorticity, of the opposite sign to the original vorticity in the cores, will be produced at the interface between the lighter exhaust gases and the surrounding air.⁵ This vorticity reduces the circulation computed on a contour passing vertically through the plane of symmetry between the vortex cores and closed on a semi-circular arc completely enclosing one vortex core and the fluid convected with it. Thus buoyancy reverses the original circulation in the wake, although it probably does not precisely cancel the flow induced by the wing.

An estimate of the distance d_b at which the cumulative buoyancy forces just equal the lift L is

$$g(H/vc_p T)d_b = L$$

or using Eq. (3)

$$d_b = \eta(L/D)(c_p T/g) \quad (6)$$

The ratio $c_p T/g$ is a characteristic length for buoyant plume and wake problems. For a typical stratospheric temperature of 210°K, $c_p T/g$ is 21.5 km. Using the above expression, d_b is 2 to 5 times $c_p T/g$ or from 40 to 100 km for most aircraft.

For most modern airplanes, d_c is much less than d_b . Thus for an unstratified atmosphere, the vortex pair will break up from the sinusoidal instability before buoyancy from the engines can overcome the initial impulse of the vortex pair.

Beyond the point at which the vortex instability occurs, the growth of the far wake will ultimately approach that of a line thermal.¹¹ In analogy to buoyant plumes, a buoyancy length l_b is defined as

$$l_b = (gH/\pi\rho c_p T v^3) \quad (7)$$

The half-width of the line thermal b is given in terms of l_b and the distance x behind the aircraft as

$$b = (3\beta/2)^{1/3} (l_b x^2)^{1/3} \quad (8)$$

in which β is an empirically determined entrainment parameter of order unity. To express the width b in a convenient dimensionless form, the length l is introduced

$$l \equiv (l_b d_b^2)^{1/3} = \left(d_b \cdot \frac{L}{\pi\rho v^2} \right)^{1/3} \quad (9)$$

Then the half-width is given as

$$\frac{b}{l} = (3\beta/2)^{1/3} (x/d_b)^{2/3} \quad (10)$$

Using a value of 0.71 for β ,^{11,†} the entrainment param-

†The entrainment parameter in Eq. (8) was determined empirically from plume rise and not by matching b to observed plume radius. Therefore b must be empirically related to the observed half-width of the wake.

eter, the half-width of the trail is of the order of l at a distance of x equal to d_b . Typical values of this radial scaling length in the far wake are 50 to 150 m .

Effects of Stratification

Atmospheric stability will limit the rise and growth of the wake. In a stably stratified atmosphere, any disturbance creates waves of a circular frequency ω , called the Brunt-Vaisala frequency

$$\omega^2 = -g(\partial \ln \rho^* / \partial z) \quad (11)$$

in which ρ^* is the potential density and z is the altitude.

For an isothermal atmosphere, an approximation valid for the lower stratosphere, $\partial \ln \rho^* / \partial z$ is the reciprocal of the scale length $c_p T / g$. The isothermal value of ω , called ω_i , is

$$\omega_i = g / (c_p T)^{1/2} \quad (12)$$

For a typical stratospheric temperature of 210°K, ω_i is 0.02 sec⁻¹.

After the vortex breaks up, the flow should approach that of a line thermal in a stratified atmosphere. Such a thermal will terminate its motion at a time π / ω^{11} . Therefore atmospheric stratification will become important at a distance d_s

$$d_s \equiv v \pi / \omega \quad (13)$$

At the point of maximum rise, the theoretical wake half-width b_{\max} will be

$$b_{\max} = \left(\frac{6 \beta l_b v^2}{\omega^2} \right)^{1/3}$$

or

$$b_{\max} / l = (6 \beta / \pi^2)^{1/3} (d_s / d_b)^{2/3} \quad (14)$$

For the first generation SST aircraft flying in the atmosphere, d_s is comparable to d_b . Therefore, b_{\max} is of the same order as the scaling length l .

If d_s is substantially less than d_b , stratification will dominate the flow before buoyancy from the exhaust does. In that case, the half-width of the wake could be significantly less than l , but it should be at least as large as the elliptical cylinder of fluid convected with the vortex pair since this is generated irrespective of buoyancy.

At distances much greater than d_s , it is unclear what motion might be observed. Hewett, Fay and Hoult¹¹ note that, at the end of the rising phase of a buoyant plume, the internal and external stratification are identical, and no further motion is observed. On the other hand, Schooley¹² proposes that gravitational collapse of aircraft wakes is important in a stratified atmosphere; that is, the wake width increases while its vertical thickness decreases. It occurs when the fluid in the wake is well mixed and, therefore, gravitationally unstable in a stratified atmosphere.

Schooley and Stewart,¹³ Schooley^{14,15} and Wu¹⁶ have modeled similar flows in the laboratory. Their results show that the characteristic time is the Brunt-Vaisala time $2\pi / \omega$. The maximum vertical thickness occurs at approximately π / ω , or at $x = d_s$, and horizontal spreading occurs for at least an order of magnitude longer.

Whether or not this wake collapse occurs depends on the internal stratification of the wake. It is conceivable that the internal stratification in the wake may result from different entrainment mechanisms. For the line thermal (Hewett, Fay, and Hoult) the entrainment may be greatest at the upper (gravitationally unstable) edge and least at the lower edge, giving rise to an internal stable stratification. On the other hand, an axisymmetric, nonbuoyant wake (Schooley and Stewart) would entrain equally around its circumference, tending to make the re-

gion more homogeneous. Wu modeled a nonturbulent, nonbuoyant wake for which no significant entrainment was observed. Until further experiments are carried out, it is probably not possible to predict which effect will dominate at distances much greater than d_s .

III. Comparison of Theoretical Models to Data on Wake Growth

In this section, data from observations of contrails from subsonic aircraft and from a laboratory experiment simulating aircraft wakes are used to verify the theoretical models of Sec. II. The contrail width data, taken from studies on military aircraft in the 1950's,^{17,18} provide field data on aircraft wake growth. Also, a model experiment was conducted to provide additional data on the growth of a buoyant aircraft wake that would not be complicated by variations in humidity, atmospheric turbulence, and stratification which influence the visibility and persistence of contrails.

Design of the Experiment

We first consider the dimensionless parameters that are important in simulating the prototype. Since this study concerns far wake development, the Mach number and the Reynolds number should not play a significant role in the development of the free shear layers in the farfield. The following parameters define the initial conditions for the development of the intermediate and far wake regimes.

Let \dot{m}_j be the mass flow of air through the aircraft engines. A thrust system scale length l_j is defined as

$$l_j = (\dot{m}_j / \rho v)^{1/2} \quad (15)$$

in which ρ and v are the freestream density and flight velocity respectively. The ratio of l_j / s is the principal dimensionless length ratio which should be simulated to model the near wake.

The downwash effects will be simulated if the lift/drag ratio, L/D , is the same for model and prototype. In addition the thrust should equal the drag.

By analogy to the simulation of buoyant plumes,¹¹ there are three additional dimensionless parameters describing the buoyant exhaust

$$\Delta_j = (T_j - T) / T \quad (16)$$

$$R = v_j / v \quad (17)$$

$$Fr = v_j / (g \Delta_j l_j)^{1/2} \quad (18)$$

The dimensionless temperature ratio Δ_j gives the relative magnitude of the temperature difference, and hence the density difference, between the jet exhaust and the atmosphere. The speed ratio R , the ratio of the jet velocity to the freestream velocity, is important in scaling the spread of the exhaust very close to the engine. The square of the Froude number Fr gives the ratio of inertial to buoyant forces at the exit of the engine.

The MIT Ship Model Towing Tank was chosen for the experiment. Large distances behind the wing are scaled by observing the wake for long periods of time. The principal advantage in water versus air is that the lower kinematic viscosity of water allows a reasonably high Reynolds number (10^4 to 10^5) to be attained with small models and low towing speeds. This value of the Reynolds number gives good lift and drag coefficients for the airfoil. Despite the large size of this tank (80 ft long, 8 ft wide, and 4 ft deep), the observation time and range of parameters was limited by interference with the free surface or the bottom.

The basic differences in the flowfields behind wings of different aspect ratios and planforms are the details of the

Table 1 Scaling parameters for aircraft and the model^a

	B-47	B-66	F-89	Concorde	Model
Span (m)	35	22	18	26	0.3
Weight (kg)	80,000	35,000	18,000	135,000	—
(L/D) cruise	14.9	13	11.9	7.7	4-30
Specific fuel consumption	1.24	1.12	1.30	1.2	—
R	2.9	3.1	2.8	1.8	1-5
l_j/s	0.037	0.037	0.039	0.07	0.04-0.08
Fr	125	215	160	230	10-30
Δ_j	2.1	2	2.2	1.4	0.005-0.20
d_c (km)	6	4	3.5	5.6	30 m
d_b (km)	54	45	40	88	3-18 m
$l(m)$	105	75	55	130	0.2-1.0 m

^a The estimates are based on a velocity of 225m/sec. and altitude of 11 km for the B-47, B-66, and F-89. The velocity of the Concorde is 650m/sec and an altitude of 16 km.

vortex roll-up which should have only minor effects on the intermediate wake. We chose a rectangular wing with a span of 1.0 ft, an aspect ratio of 4 and a NACA 63A010 airfoil. It was mounted at a geometric angle of attack of 7° on a streamlined strut. The distance from the bottom of the tank to the airfoil varied from 1.7 to 2.2 ft.

To simulate the engine exhausts, two small jets made from 1/4 in. copper elbows were mounted at the one-quarter span positions in holes through the wings such that the axes of the jets were parallel to the direction of travel and 1/2 in. beneath the trailing edge. Fluid was supplied to these jets through streamlined tubes that were vertical and parallel to the support strut.

A denatured alcohol-water mixture, dyed with blue ink, simulated the buoyancy of the exhaust. Since the buoyancy in the wake is produced by a lighter, miscible fluid instead of excess temperature, the dimensionless temperature ratio is redefined in terms of density as $\Delta_j = (\rho_w - \rho_j)/\rho_w$ in which ρ_w and ρ_j are the densities of the water in the towing tank and of the alcohol-water solution respectively. These densities were determined using hydrometers. The product of this ratio Δ_j and the total flow rate of the jets is the buoyancy flux which is equivalent to $gH/\pi\rho c_p T$ in the definition of the buoyancy length l_b [Eq. (7)]. Red ink was injected into the flow from small tubes in the wing tips to visualize the vortex cores.

The growth and rise of the wake and the motion of the vortices were recorded with two 35 mm still cameras and a motion picture camera. One 35 mm camera was mounted over the center of the tank 4 ft from the surface of the water; the other camera, mounted 5 ft from the side of the tank viewed the motion through a large window. Their respective fields of view covered nearly the entire width and depth of the tank at the observing station. These cameras were fired simultaneously at specified intervals after the passage of the airfoil. The motion picture camera was used to obtain an over-all impression of the vortex instability and the interaction between the exhaust jets and the vortices. Further details of the experiment are given by Overcamp.¹⁹

Experimental Results

For these tests the predominate form of vortex dissipation was not the sinusoidal instability often observed in the field, but rather, vortex bursting in which the vortex cores abruptly increase in diameter and dissipate rapidly.

The bursting instability is thought to be caused by axial flow within the swirling vortex core.²⁰ In some of the experiments, axial flow was observed by pulsing the red ink marking the core. At a distance of about two spans downstream, the axial flow relative to the tank was found to be directed back toward the wing. Estimates of the axial velocity for three runs are 10 to 20% of the speed of the

wing. This is in agreement with towing tank studies by Olsen²¹ and by Bilanin and Widnall.²²

Table 1 gives estimates of the dimensionless variables that define the near wake and the characteristic length scales for the Concorde, the three subsonic airplanes used in the contrail studies, and the range of values of the experiments.

The large value of Δ_j , typical of these turbojet aircraft, can not be attained with the alcohol-water solution since the value of Δ_j is only 0.2 for pure alcohol. Since towing tank tests simulating buoyant plumes have shown that the farfield results were insensitive to changes in Δ_j over a range from 0.1 to 0.4²³, we feel that this was probably a small effect on the farfield results in these experiments also.

The Froude number is up to an order of magnitude too low in some of the tests. It was noted that for tests with Froude number of 10, the jet exhausts quickly rose above and were not significantly influenced by the vortex system. Data for these tests are not presented.

The experiments also differ from actual aircraft in that there was no attempt to keep thrust equal to drag. The thrust to drag ratio varied from 0.5 to 5 in the experiments. Except for the effect of high thrust on the vortex bursting, no changes of the wake behavior with thrust were observed.

For correct interpretation of the data, two definitions must be made. The observed horizontal width of the region of the wake marked either by the dye of the exhaust fluid, as in the laboratory experiments, or by visible con-

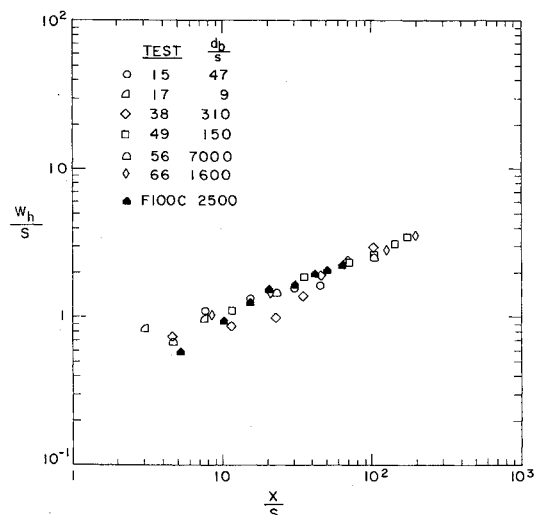


Fig. 1 Dimensionless wake width, w_h/s , vs. dimensionless downstream distance, x/d_c , for the intermediate wake.

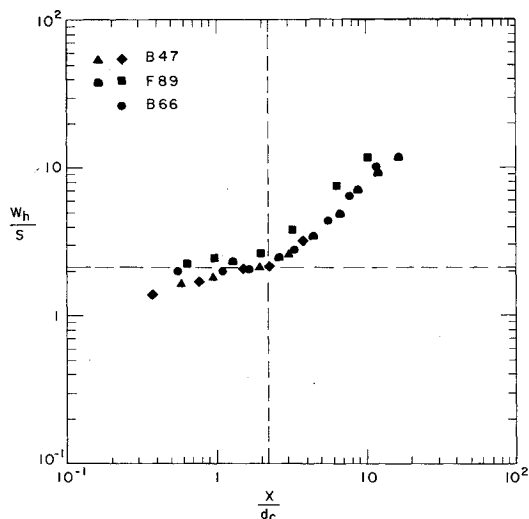


Fig. 2 Dimensionless wake width, w_h/s , vs. dimensionless downstream distance, x/d_c , for the intermediate wake.

densed water or ice crystals, as for contrails, is termed the wake width w_h . The observed vertical thickness is called the wake thickness and is denoted by w_v .

Figure 1 shows the data for a number of experiments on the observed width w_h plotted against the downstream distance x , both nondimensionalized by the wing span s . Only those points for which x is less than d_b are presented. Next to each symbol is the value of d_b/s for that experiment. The slope of this data on the log-log plot is 0.35, suggesting a wake-like behavior of the flow.

Data from Smith and Diamond's¹⁷ Fig. 6 for the width of the contrail of an F100C (a small, single-engine fighter) is also plotted on Fig. 1. This shows that the transition from the near wake, characterized by individual exhaust streams, to the intermediate wake, dominated by the vortex pair, exhibits this wake-like growth.

The model chosen for the intermediate region is the classical vortex pair. Since vortex bursting prematurely dissipated the vortex pair in these experiments, the laboratory data did not show the dominance of the vortex pair. Figure 2 shows this effect for the contrail data. The wake width divided by the wing span is plotted versus the downstream distance x divided by the scaling length d_c . At early distances the width grows to about the size of the fluid convected with the pair, indicated by the dashed

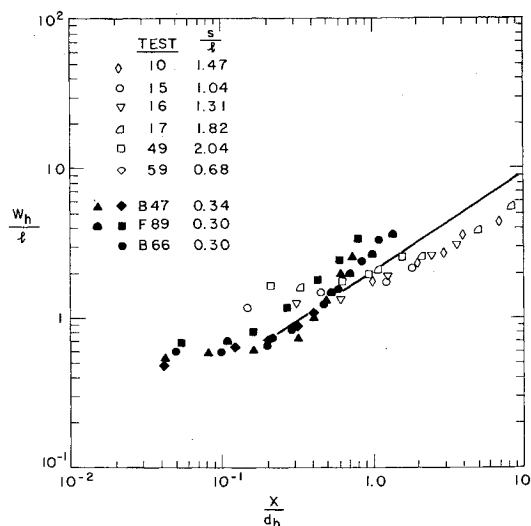


Fig. 3 Dimensionless wake width, w_h/l , vs. dimensionless downstream distance, x/d_b , for the far wake. Solid line is the assumption that the visible width of the wake is of the order of $2b$.

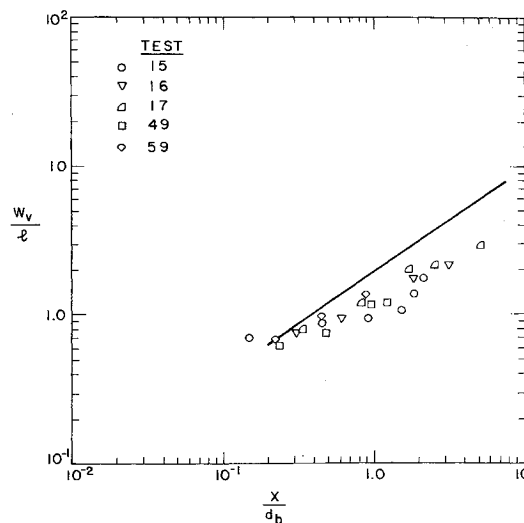


Fig. 4 Dimensionless wake thickness, w_v/l , vs. dimensionless downstream distance, x/d_b , for the far wake. Solid line is the assumption that the visible thickness is of the order of $2b$.

horizontal line. Then the width remains nearly constant until the sinusoidal instability breaks up the pair. The dashed vertical line is the distance ($2.2d_c$) found by Condit and Tracy¹⁰ for this instability. The agreement between the proposed model for the intermediate wake and the field data is good.

At distances longer than this, the buoyancy of the exhaust is expected to play a major role. The actual width, therefore, is compared to the width of the line thermal model. Several investigators have recently made such observations for laboratory experiments that give a correlation between observed width of line thermals and the theoretical width b . Hewett, Fay, and Hoult¹¹ found that the half-width of the vertical temperature profile of a buoyant plume rising in a stably stratified atmosphere to be $1.2b$ where b is given by Eq. (8). Tsang's²⁴ data for a buoyant line thermal in an unstratified tank showed that the radius of an equivalent circular plume, i.e., a circle with the same cross-sectional area as the visible thermal, to be $0.75b$. Therefore we felt that the visible width and thickness should be of the order of $2b$.

The visible width and distance downstream, nondimensionalized by l and d_b respectively, for both the laboratory and contrail experiments, is given in Fig. 3. The straight line is our assumption that the total visible width w_h is $2b$.

The field data have a width of $0.6l$ for distances short compared to d_b . This corresponds to the intermediate wake regime where the visible width was observed to be twice the wing span which is about $0.3l$ for all three aircraft. For longer distances, the observed width grows at a slightly faster rate than the two-thirds power law for a thermal. At a distance equal to d_b , the visible width is slightly greater than $2b$, i.e., the width is approximately equal to the line thermal model chosen to represent the growth of the buoyant wake.

The behavior of the laboratory data of wake widths is somewhat different from the field results. At short distances compared to d_b , the widths are slightly larger than l because these experiments had a ratio of s/l of about unity. For all experiments with ratios of s/l comparable to real airplanes, no measurements could be made for distances much larger than d_b due to interference of the wake with the bottom of the tank. For distances much larger than d_b , the width is proportional to $2b$, i.e., it follows the two-thirds growth law for a buoyant thermal. Similar behavior of the vertical thickness is given in Fig. 4.

The differences between the field and laboratory results

Table 2 Radiative heating in the stratosphere for July, 40°N

Pressure mb	Altitude km	O ₃ -UV °K/day	O ₃ -9600 nm °K/day	H ₂ O °K/day	CO ₂ °K/day	NIR °K/day
100	16	+0.157	+0.272	-0.176	-0.244	+0.191
70	18	+0.352	+0.369	-0.223	-0.562	+0.201
50	21	+0.712	+0.344	-0.253	-0.981	+0.217
30	24	+1.286	+0.180	-0.286	-1.407	+0.240
20	27	+1.795	-0.005	-0.307	-1.883	+0.265

in the far wake shown in Fig. 3 have not been completely explained. Several additional effects have been investigated. The first is the buoyancy added to the wake due to the condensation and freezing of the water vapor in forming the visible contrails. If all the water vapor condenses, the percentage increase of buoyancy is the percentage difference between the higher and lower heating value of the fuel or roughly 5%. If the water freezes, another small fraction of additional buoyancy will be released. Both these factors cannot give the differences seen in Fig. 5.

Atmospheric turbulence, shear, or stratification will play a role in the contrail data. Unfortunately these quantities were not measured.

Our conclusions for the growth of an aircraft wake are: (1) both the contrail data and the model experiments scale with the characteristic buoyant length l and distance d_b ; (2) the magnitude of the width in the far wake is predicted by the buoyant thermal model, and, (3) the data show a faster rate of growth in the farfield than would have been expected for a wake without buoyancy.

IV. Subsidence of the Wake

The previous sections show that the growth of an aircraft wake due to the aerodynamic effects of lift, drag, and buoyancy is limited by stable stratification. Also stable stratification would limit atmospheric turbulence, making further dispersion of the exhaust products a slow process. These observations lead to the speculation that the exhaust products of an SST or any aircraft flying in the stratosphere may slowly sink due to differential radiative heating of the wake.

The rest of this paper presents a model calculating the photochemistry, radiation, and dispersion of the wake. It shows that the wake region will subside if the dispersion is slow and if there is local ozone destruction.

Equation (14) predicts the maximum half-width b_{\max} as a function of the characteristic radial dimension of the wake l , the buoyancy length d_b , and the stratification length d_s . For the Concorde, the length l is estimated to be 130 m, and d_b is 88 km. For its cruise altitude and speed, d_b is around 90 km. From Eq. (14), the maximum theoretical half-width of the wake is of the order of 100 m; hence, the diameter is about $2b_{\max}$ or 200 m.

Since the Concorde's weight is about one-half of the design weight of the Boeing SST, the emissions of water vapor, carbon dioxide, and the oxides of nitrogen were assumed to be one-half of the estimates given by Johnston^{1,2} or 440 kg/hr per aircraft. In addition, this was reduced in one case (case 2) by a factor of ten to test the sensitivity of the model to NO_x emitted.

Based on these estimates of wake diameter and NO_x emission, the average concentration of NO_x in the wake will be 1.2×10^{11} molecules/cm³ in case 1 and 1.2×10^{10} molecules/cm³ in case 2.

Photochemistry of Ozone

The photochemical model used for the calculation of ozone depletion by NO_x in the aircraft's wake is based on

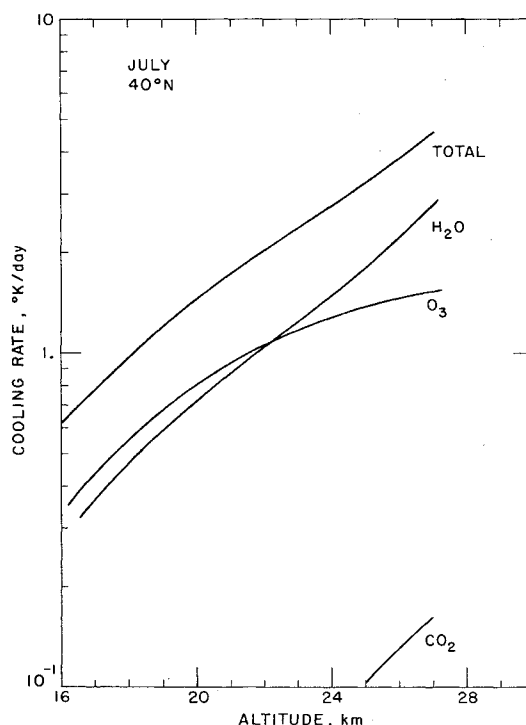


Fig. 5 Relative cooling rate of the wake vs altitude for July, 40°N.

the following set of reactions^{1,2}

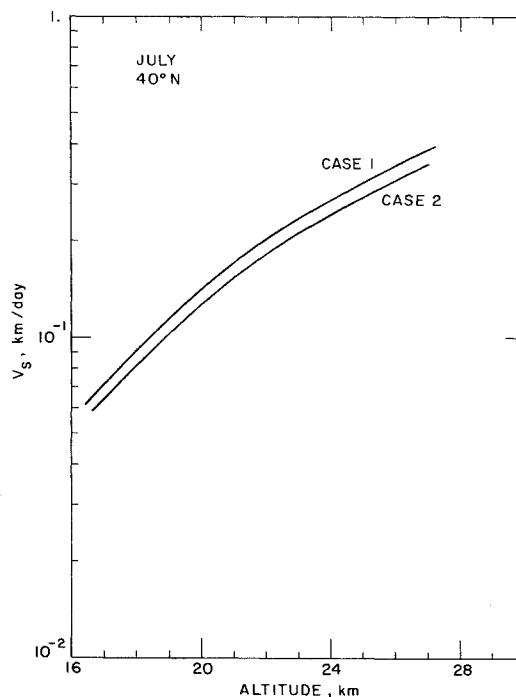
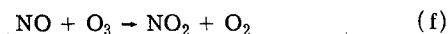
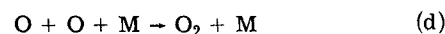
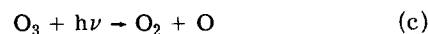
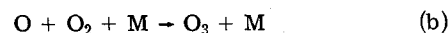
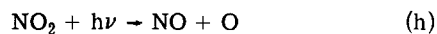
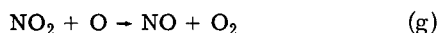


Fig. 6 Wake subsidence velocity vs altitude for July, 40°N.



The reactions (a-e) are the classical Chapman reactions for ozone. Reactions (f-h) are the fast NO_x reactions that deplete ozone.

The rate of destruction of "odd oxygen" (O and O_3) is given by

$$\frac{d}{dt}([\text{O}] + [\text{O}_3]) = 2j_a[\text{O}_2] - 2\phi k_e[\text{O}_3][\text{O}] \quad (19)^*$$

in which ϕ , the catalytic ratio, is defined as

$$\phi = 1 + \frac{k_g[\text{NO}_2]}{k_e[\text{O}_3]} = 1 + \frac{[\text{NO}]k_f k_g / k_e j_h}{1 + k_g[\text{O}]/j_h} \quad (20)$$

Since $[\text{O}_3] \gg [\text{O}]$ in the lower stratosphere, Eq. (19) is essentially the change in ozone.

The half-time for the destruction of ozone in the presence of the catalyst NO_x is

$$\tau_{1/2} = \ln 2 / 2k_e[\text{O}]\phi \quad (21)$$

The effect of the NO_x is to speed the reaction by a factor of ϕ and decrease the final ozone by a factor of $\phi^{-1/2}$.

A sample calculation shows the importance of NO_x . At 15 km $[\text{O}]$ is 10^6 molecules/cm³. If $[\text{NO}_x]$ is 10^{11} molecules/cm³ the catalytic reduction rate ϕ is 290 and $\tau_{1/2}$ is 1.3×10^6 sec in contrast to 10^8 sec for the pure oxygen system.

Radiation

High concentrations of exhaust gases will also cause changes in the radiation balance of the wake region. If the ozone is depleted, there will be less heating of this region due to the photolysis of ozone by UV radiation. Also large excess of water vapor in the wake compared to the natural levels in the stratosphere will cause additional infrared cooling in the rotational water vapor bands.

Calculation of the cooling from ozone is relatively simple. Given the final wake size and NO_x emissions, the new level of ozone is calculated. The solar heating of the remaining ozone is proportional to the new level of ozone, i.e., a 90% reduction in ozone implies that the solar heating will be 10% of its original value, and the relative cooling of the wake will be 90% of the original heating value.

Dopplick²⁵ recently made extensive calculations for the radiative heating of the earth's atmosphere. Table 2 gives his calculated heating rates for 40°N for July. Radiative heating rates from ozone at 100 mb (16 km) are around 0.2°K/day and are about 2°K/day at 20 mb (27 km).

Ozone has an important radiation band in the far infrared at 9600 nm which heats the atmosphere between 10 and 25 km at midlatitudes. Again the ozone deficit causes a relative cooling of the wake, and it is calculated in the same manner as are the solar heating bands.

For a wake with an average diameter of 200 m, the water vapor concentration will exceed the ambient levels and cause additional differential cooling. We assume that the total cooling rate will be assumed proportional to water vapor concentration because the radiational cooling of water vapor in the stratosphere is primarily due to radiational transfer directly to space instead of radiational exchange to the ground or to other levels in the atmosphere,²⁶ and it can be shown that there is so little water vapor above any level in the stratosphere that the weak line approximation for radiation between the stratosphere and space is valid. Then the local emissivity is directly proportional to the local number density of water vapor.

Cooling from excess CO_2 in the 1500 nm band is treated in the same manner as the water vapor, but its contribution is much smaller because the excess CO_2 in the wake is only a small percentage of the ambient concentration.

The final contribution to the calculation of the relative cooling rate is the absorption of the near infrared radiation (NIR) from the sun. The principal absorbers are CO_2 , H_2O , and O_2 . Yamamoto²⁷ shows that, throughout the lower stratosphere, CO_2 absorption is larger than the heating due both to water vapor and oxygen. Since Table 2 shows that the near infrared heating is normally only 0.2°K/day at this latitude, the heating due to the excess CO_2 and H_2O is not included. This will be a good approximation at 15 km, but will be worse at higher altitudes due to a larger excess of water vapor.

The rate of subsidence of the wake is calculated from the differential cooling rate C_r and the gradient of potential temperature. The velocity v_s is

$$v_s = C_r / (\partial T^* / \partial z) \quad (22)$$

This assumes that the wake will always sink to remain in equilibrium.

Calculations of Wake Subsidence

Calculations for the sinking velocity were made for a Concorde size aircraft. The altitude range extended from 16 to 27 km to cover the cruise altitudes of the Concorde and Tupolev 144 aircraft, and possible future aircraft. These calculations were based on the two assumed emission rates of NO_x , a final wake diameter of 200 m, Dopplick's calculations for the months of January and July at 20°N, 40°N, and 60°N, the standard atmospheres for 15°N, 45°N, 60°N²⁸, and a water vapor mixing ratio of 2×10^{-6} kg/kg. The natural ozone level was taken from Dopplick; the atomic oxygen levels were taken from Johnston. They assume that there is no further dispersion of the exhaust gases, and therefore set an upper limit to the rate of subsidence for the wake.

The calculation of the ozone depletion for the NO_x emissions corresponding to Johnston's report, 440 kg/hr per aircraft, show that the ozone level in the wake region will be reduced to 0.05 to 0.12 of its original concentration. For the low emission case, 44 kg/hr per aircraft, the ozone is reduced to 0.2 to 0.35 of the original amount. The half-time for ozone depletion $\tau_{1/2}$ is substantially reduced in the wake. For July, 40°N and the high emissions case, $\tau_{1/2}$ is 5×10^5 sec compared to 6×10^8 for pure oxygen. At 27 km, $\tau_{1/2}$ is 2×10^3 sec compared to 1.5×10^5 sec. With the low emission case, the half-time is a factor of ten higher than the high emission case.

Figure 5 shows the cooling rate calculations for July, 40°N and the high emission level of NO_x (case 1). At low altitudes ozone and water vapor have nearly equal contributions to the cooling. At altitudes above 22 km, the water vapor cooling exceeds the ozone. Carbon dioxide contributes very little to the cooling rate at any altitude. The calculations for 20°N and 60°N are within a factor of two of those for July, 40°N except for January, 60°N when the days are short, and the normal heating by ozone falls to nearly zero.

The descent velocity of the wake region is given in Fig. 6 for both cases on July at 40°N. At 16 km v_s is 0.06 km/day and rises to 0.4 km/day at 27 km. Thus at the cruise altitudes of the first generation SST's, the descent rate is slow.

Effect of Atmospheric Turbulence

Dispersion of the wake by atmospheric turbulence can slow this subsidence considerably. If the dispersion is fast, the NO_x from each SST will be quickly spread over such a

* k_i is the rate constant for the i th reaction

large volume of the stratosphere that there will be no local depletion of ozone and no sinking.

Unlike the first several hundred meters of the earth's atmosphere, very little is known of the characteristics of turbulence in the stratosphere. Some of the only sources are the global diffusion studies of trace constituents in the upper atmosphere. This diffusion occurs over very long time and length scales compared to the aircraft wake, and therefore, the diffusion coefficients are not directly applicable to this local dispersion problem.

We make use of Richardson's similarity theory²⁹ to scale the global coefficients to the local dispersion of the wake. This theory says that K , the dispersion coefficient, should vary in proportion to $x^{4/3}$ where x is the separation of two particles in a turbulent field. This suggests that, for the aircraft wake, the local dispersion coefficient should vary as $d^{4/3}$ where d is an average diameter based on concentration.

Gudiksen, Fairhall and Reed³⁰ give global eddy diffusion coefficients found from a study of the diffusion of radioactive tungsten from nuclear tests. The values for the vertical diffusion coefficient at 27 km varied from 3×10^2 to 6×10^3 cm²/sec. At 15 km, the coefficient ranged from 10^3 to 1.3×10^4 cm²/sec. The global horizontal diffusion coefficients ranged from 5×10^8 to 6×10^9 cm²/sec. Since the horizontal diffusion is caused by large eddies with diameters of the order of 10^2 to 10^3 kilometers, these eddies will not cause dispersion on length scales of the order of hundreds of meters. Using Richardson's scaling law, a local dispersion coefficient would be at least four orders of magnitude smaller than these horizontal diffusion coefficients or 10^5 to 10^6 cm²/sec. This probably sets an upper bound for the initial dispersion of the wake. On the other hand, the global dispersion in the vertical is caused by smaller scale eddies, which are more comparable to the size of the wake. Its value of 10^2 to 10^4 cm²/sec may indicate a lower limit.

We present two calculations to illustrate how atmospheric turbulence will modify the sinking for both a low dispersion coefficient (10^5 cm²/sec) for altitudes of 16 and 27 km.

At 27 km all the factors for subsidence are favorable. The descent velocity is high, the half-times for the reactions are fast, and the average dispersion coefficient will probably be low since atmospheric stability increases with altitude.

Consider the time it takes for the average diameter of the wake to grow from 200 m to 1000 m. Since at the latter point the concentrations of NO_x and H₂O will be reduced by a factor of 25, the relative cooling rate will go to zero, and the half-time for the ozone depletion will be long. The characteristic time for this dispersion to occur is given by

$$\tau_d = d^2/K \quad (23)$$

For $K = 10^3$ cm²/sec, τ_d is 10^7 sec which is significantly greater than both the half-time for ozone at 27 km and the time for the wake to descend many kilometers. If K is 10^5 cm²/sec, τ_d is 10^5 sec or about one day, and the total subsidence would be less than a few hundred meters.

At 16 km, the rate of sinking was calculated to only be 0.06 km/day. If the local dispersion coefficient were to be as low as 10^3 cm²/sec, the wake would remain sufficiently small so that the ozone depletion could occur and subsidence begin. But as it did sink the differential cooling would decrease due to the increase in water vapor and decrease in ozone at lower altitudes. The total subsidence would at best be a kilometer or two. If K is 10^5 cm²/sec or greater, the exhaust products would be dispersed before any ozone depletion or subsidence could occur.

V. Conclusions

The theoretical models of wake development point out two characteristic regimes in the early history of the wake of a jet aircraft. The first is the intermediate wake, dominated by the trailing vortex pair. After this pair dissipates due to the sinusoidal instability, the buoyancy from the excess heat released by the engines controls the flow. The wake growth approaches that of a line thermal. In a stably stratified atmosphere, the growth of the wake is limited, and it is predicted as a function of the stratification and aircraft parameters. Experimental data from field observations of contrails and from a laboratory experiment verify this model for a neutral atmosphere.

For the case of no atmospheric dispersion, the model of wake subsidence shows that the exhaust gases will sink from the differential cooling of the gases due to the depletion of ozone from the NO_x in the wake and to the high concentration of water vapor. Dispersion by atmospheric turbulence will slow and eventually stop this sinking. Although little is known about the actual atmospheric dispersion in the stratosphere, estimates show that if the turbulence is weak, the subsidence can continue for days to weeks. For stronger turbulence, the dispersion will prevent the process entirely.

Wake subsidence will probably not be an effective mechanism for the present generation of SST's at altitudes of 16–18 km in the stratosphere. For future aircraft flying at higher altitudes, the wake has the potential of sinking several kilometers to the lower regions of the stratosphere but certainly no lower than 16–20 km. This may be important because it would reduce the residence time of the nitric oxides in the stratosphere which would moderate the environmental effects of these aircraft.

References

- ¹Johnston, H., "Reduction of Stratospheric Ozone by Nitrogen Oxide Catalysts from Supersonic Transports," *Science*, Vol. 173, 1971, pp. 517–522.
- ²Johnston, H., "Catalytic Reduction of Stratospheric Ozone by Oxides of Nitrogen," Rept. 20568, 1971, University of California Radiation Laboratory, Berkeley, Calif.
- ³Wilson, C. L., ed., *Inadvertent Climate Modification*, MIT Press, Cambridge, Mass., 1971, pp. 258–291.
- ⁴Crow, S., "Stability Theory for a Pair of Trailing Vortices," *AIAA Journal*, Vol. 8, No. 12, Dec., 1970, pp. 2172–2179.
- ⁵Scorei, R. S. and Davenport, L. J., "Contrails and Aircraft Downwash," *Journal of Fluid Mechanics*, Vol. 43, Sept. 1970, pp. 451–464.
- ⁶Tombach, I. H., "Transport of a Vortex Wake in a Stably Stratified Atmosphere," *Aircraft Wake Turbulence and Its Detection*, edited by J. H. Olsen, A. Goldburg and M. Rodgers, Plenum Press, New York, 1971, pp. 41–56.
- ⁷Saffman, P. G., "The Motion of a Vortex Pair in a Stratified Atmosphere," 24th Annual Meeting of the Division of Fluid Dynamics of the American Physical Society, San Diego, 1971.
- ⁸Heywood, J. B., Fay, J. A., and Linden, L. H., "Jet Aircraft Air Pollutant Production and Dispersion," *AIAA Journal*, Vol. 9, No. 5, May 1971, pp. 841–850.
- ⁹Lamb, H., *Hydrodynamics*, 6th ed., Cambridge University Press, Cambridge, Mass., 1932, Section 155, pp. 220–224.
- ¹⁰Condit, P. H. and Tracy, P. W., "Results of the Boeing Company Wake Turbulence Test Program," *Aircraft Wake Turbulence and Its Detection*, edited by J. H. Olsen, A. Goldburg, and M. Rodgers, Plenum Press, New York, 1971, pp. 473–508.
- ¹¹Hewett, T. A., Fay, J. A., and Hoult, D. P., "Laboratory Experiments of Smokestack Plumes in a Stable Atmosphere," *Atmospheric Environment*, Vol. 5, Sept. 1971, pp. 767–789.
- ¹²Schooley, A. H., "Airplane Contrails Related to Vertical Wake Collapse," *Bulletin of the American Meteorological Society*, Vol. 50, 1969, p. 719.
- ¹³Schooley, A. H. and Stewart, R. W., "Experiments with a Self-propelled Body Submerged in a Fluid with a Vertical Density Gradient," *Journal of Fluid Mechanics*, Vol. 15, 1963, pp. 82–96.
- ¹⁴Schooley, A. H., "Wake Collapse in a Stratified Fluid," *Science*, Vol. 157, 1967, pp. 421–423.

- ¹⁵Schooley, A. H., "Wake Collapse in a Stratified Fluid: Experimental Exploration of Scaling Characteristics," *Science*, Vol. 160, 1968, pp. 763-764.
- ¹⁶Wu, J., "Mixed Region Collapse with Internal Wave Generation in a Density Stratified Medium," *Journal of Fluid Mechanics*, Vol. 35, 1969, pp. 531-544.
- ¹⁷Smith, T. B. and Diamond, R. J., "Studies of Contrails from Jet Powered Aircraft," Final Rept. Contract AF19(604)-1495, 1955, Meteorology Research, Inc., Pasadena, Calif.
- ¹⁸Smith, T. B. and Beesmer, K. M., "Contrail Studies for Jet Aircraft," Final Report Contract AF19(604)-2038, 1959, Meteorology Research, Inc., Pasadena, Calif.
- ¹⁹Overcamp, T. J., "Dispersion of the Exhaust of a Supersonic Transport in the Stratosphere," Ph.D. thesis, Massachusetts Institute of Technology, Dept. of Mechanical Engineering, Cambridge, Mass., Feb. 1973.
- ²⁰Landahl, M. T. and Widnall, S. E., "Vortex Control," *Aircraft Wake Turbulence and Its Detection*, edited by J. H. Olsen, A. Goldburg, and M. Rogers, Plenum Press, New York, 1971, pp. 137-155.
- ²¹Olsen, J. H., "Results of Trailing Vortices in a Towing Tank," *Aircraft Wake Turbulence and Its Detection*, edited by J. H. Olsen, A. Goldburg, and M. Rogers, Plenum Press, New York, 1971, pp. 455-472.
- ²²Bilanin, A. J. and Widnall, S. E., "Aircraft Wake Dissipation by Sinusoidal Instability and Vortex Breakdown," AIAA Paper No. 73-107, Washington, D.C., 1973.
- ²³Hoult, D. P. and Weil, J. C., "Turbulent Plume in a Laminar Cross Flow," *Atmospheric Environment*, Vol. 6, 1972, pp. 513-532.
- ²⁴Tsang, G., "Laboratory Study of Line Thermals," *Atmospheric Environment*, Vol. 5, 1971, pp. 445-471.
- ²⁵Dopplick, T. G., "Global Radiative Heating of the Earth's Atmosphere," Planetary Circulation Project Rept. 24, 1970, Department of Meteorology, MIT, Cambridge, Mass.
- ²⁶Rodgers, C. D. and Walshaw, C. D., "The Computation of Infrared Cooling Rate in Planetary Atmospheres," *Quarterly Journal of the Royal Meteorological Society*, Vol. 92, 1966, pp. 67-92.
- ²⁷Yamamoto, G., "Direct Absorption of Solar Radiation by Water Vapor, Carbon Dioxide, and Molecular Oxygen," *Journal of the Atmospheric Sciences*, Vol. 19, 1962, pp. 182-190.
- ²⁸U.S. Standard Atmosphere Supplements, 1966, U.S. Government Printing Office, Washington, D.C., 1966, Part 5.
- ²⁹Sutton, O. G., *Micrometeorology*, McGraw-Hill, New York, 1953, pp. 319-322.
- ³⁰Gudiksen, P. A., Fairhall, A. W., and Reed, R. J., "Roles of Meridional Circulation and Eddy Diffusion in the Transport of Trace Substances in the Lower Stratosphere," *Journal of Geophysical Research*, Vol. 73, 1968, pp. 4461-4473.

DECEMBER 1973

J. AIRCRAFT

VOL. 10, NO. 12

Flutter of Pairs of Aerodynamically Interfering Delta Wings

Richard R. Chipman,* Frank J. Rauch†
Grumman Aerospace Corporation, Bethpage, N.Y.

AND

Robert W. Hess‡
NASA Langley Research Center, Hampton, Va.

To examine the effect on flutter of the aerodynamic interference between pairs of closely spaced delta wings, several structurally uncoupled 1/80 th-scale models were studied by experiment and analysis. Flutter test boundaries obtained in NASA Langley's 26-in. transonic blowdown wind tunnel were compared with subsonic analytical results generated using the doublet lattice method. Trends for several combinations of vertical and longitudinal wing separation were determined, showing flutter speed significantly affected in the closely spaced configurations. For some configurations, a flutter mechanism coupling flexible modes of both surfaces at a disinctive flutter frequency was predicted and observed. The flexibilities of both surfaces were concluded to be essential to the analysis.

Nomenclature

b_r	= reference semi-chord of trailing wing	q	= displacement vector of the degrees of freedom
c	= mean aerodynamic chord of leading wing	Q	= aerodynamic force vector
f	= frequency, Hz	V_f	= flutter velocity
g	= damping	$V_f(\infty)$	= V_f of flutter-critical isolated wing
h	= biplanar (vertical) wing separation	$V_f(h, l)$	= V_f of a configuration with biplanar and streamwise separations, h and l
k	= stiffness matrix	μ	= mass density ratio
l	= streamwise (longitudinal) wing separation	ω_f	= flutter frequency, rad./sec.
m	= mass matrix	ω_r	= reference frequency
M	= Mach number		

Presented as Paper 73-314 at the AIAA Dynamics Specialists Conference, Williamsburg, Virginia, March 19-20, 1973; submitted April 11, 1973; revision received July 23, 1973. This work was performed under NASA Contract NAS 1-10635-7. The Authors wish to acknowledge the assistance of E. Pasyanos, Grumman Aerospace Corporation, in the performance of the flutter analyses.

Index categories: Aeroelasticity and Hydroelasticity; Aircraft Testing (Including Component Wind Tunnel Testing); Spacecraft Configurational and Structural Design (Including Loads).

*Aeroelasticity Method Engineer.

†Dynamics Engineer.

‡Aerospace Research Engineer.

Introduction

THE aerodynamic interaction of lifting surfaces in proximity can create aerodynamic forces sufficient to destabilize surfaces otherwise flutter-free within their flight envelope. This problem on various aircraft designs has stimulated the efforts of several investigators: T-tail flutter was found to be a problem by Stahle.¹ To predict unsteady aerodynamic loads on a T-tail, Stark² subsequently developed a subsonic nonplanar doublet-lattice theory. Similarly, Laschka³ extended the so called kernel function method to multiple coplanar surfaces. Experiments re-